ARTICLES

Journal of Semiconductors
(2021) 42, 092001
doi: 10.1088/1674-4926/42/9/092001

Synthesis of two-dimensional/one-dimensional heterostructures with tunable width

Di Wang, Zucheng Zhang, Bo Li, and Xidong Duan†

Hunan Key Laboratory of Two-Dimensional Materials, State Key Laboratory for Chemo/Biosensing and Chemometrics, College of Chemistry and Chemical Engineering, Hunan University, Changsha 410082, China

Abstract: Two-dimensional/one-dimensional (2D/1D) heterostructures as a new type of heterostructure have been studied for their unusual properties and promising applications in electronic and optoelectronic devices. However, the studies of 2D/1D heterostructures are mainly focused on vertical heterostructures, such as MoS_2 nanosheet-carbon nanotubes. The research on lateral 2D/1D heterostructures with a tunable width of 1D material is still scarce. In this study, bidirectional flow chemical vapor deposition (CVD) was used to accurately control the width of the WS_2/WSe_2 (WS_2/MoS_2) heterostructures by controlling reacting time. WSe_2 and MoS_2 with different widths were epitaxially grown at the edge of WS_2, respectively. Optical microscope, atomic force microscope (AFM), and scanning electron microscope (SEM) images show the morphology and width of the heterostructures. These results show that the width of the heterostructures can be as low as 10 nm by using this method. The interface of the heterostructure is clear and smooth, which is suitable for application. This report offers a new method for the growth of 1D nanowires, and lays the foundation for the future study of the physical and chemical properties of 2D/1D lateral heterostructures.

Key words: chemical vapor deposition (CVD); 2D/1D heterostructures; width control

Citation: D Wang, Z C Zhang, B Li, and X D Duan, Synthesis of two-dimensional/one-dimensional heterostructures with tunable width[J]. *J. Semicond.*, 2021, 42(9), 092001. http://doi.org/10.1088/1674-4926/42/9/092001

1. Introduction

Nanowires, as a kind of one-dimensional (1D) nanostructure, have been studied for many years. As early as 1995, William *et al.* has synthesized InP, InAs, and GaAs nanowhiskers by a solution–liquid–solid method[1]. In the following decades, more and more studies on nanowires have been reported, such as electrical properties[2–4], synthesis methods[5–8], theoretical prediction[9–12] and so on. Due to the quantum size effect and edge effect, the 1D materials show many different properties compared to 2D nanosheets. For example, zigzag graphene nanoribbons with a narrow width are antiferromagnetic semiconductors, while a semiconductor-to-metal transition can be observed as the width increases[13]. Recent reports show that 1D InSe nanowires, synthesized by a physical vapor transport system or chemical vapor deposition (CVD) method, exhibit high photoresponsivity and fast response speed due to the enhanced density of states[10, 14].

The problem of lattice mismatch is often faced when 2D materials are combined into a heterostructure, but the appearance of 1D nanowires solves this problem. Recently, heterostructures composed of 1D materials and 2D materials have attracted much attention due to their promising application in electronic and optoelectronic devices. For instance, Qin *et al.* reported the synthesis of 1D Mo_6Te_6–2D $MoTe_2$ heterostructures via the molecular beam epitaxy (MBE) method, which provides a new approach to synthesize 1D semimetallic nanowires[15]. Moreover, 2D/1D heterostructures have exhibited excellent device performances in many reports, such as high on/off ratio[16], wide gate tunability[17], better performance in lithium-ion batteries[18] and remarkable hydrogen evolution reaction (HER) activity[19]. However, previous studies of 2D/1D heterostructures are mainly focused on vertical stacking. Controllable synthesis of 2D/1D lateral heterostructures with tunable width is rarely reported.

Herein, we successfully synthesize 2D/1D WS_2/WSe_2 (WS_2/MoS_2) lateral heterostructures via a home-built bidirectional airflow CVD reactor in which the width of the WSe_2 (MoS_2) can be controlled by controlling air flow direction and growth time. Scanning electron microscope (SEM) and atomic force microscopy (AFM) images show that the width of the WSe_2 can be tuned from 11 nm to 4 μm by precisely controlling the growth time. The interface of the 2D/1D heterostructures is clear and sharp. We also control the width of MoS_2 in the same way. Our research provides a new method for the synthesis of 1D nanowires and lays the foundation for the future study of 2D/1D lateral heterostructures.

2. Methods

2.1. Synthesis of 2D WS_2

WS_2 nanosheets were first synthesized as substrates in our experiment. Different from the traditional CVD system, our reactor is equipped with four switches, which can pass two directions of air flow. At first, the WS_2 powders were used as precursor and placed in the center of the heat zone. Meanwhile, the SiO_2 (285 nm)/Si was placed at the low temperature zone. Next, 600 sccm Ar gas was introduced from the substrate to the precursor (green arrow, reverse flow) for about 20 min to clean the air in the quartz tube. Then, the

Correspondence to: X D Duan, xidongduan@hnu.edu.cn
Received 7 APRIL 2021; Revised 21 APRIL 2021.

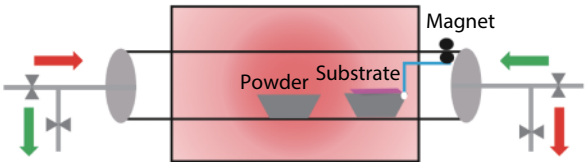

Fig. 1. (Color online) Schematic of a modified bidirectional flow CVD system.

flow rate was reduced to 75 sccm and the furnace was heated to 1200 °C in 40 min. When the temperature reached 1200 °C, we changed the direction of Ar gas to forward (red arrow) and kept it for 4 min. At last, the reactor was cooled to room temperature.

2.2. Synthesis of 2D/1D WS_2/WSe_2 heterostructures

At first, the WSe_2 powders, as the precursor, were placed in the center of the heat zone. The SiO_2/Si substrate with WS_2 nanosheets was placed in the low temperature zone to grow heterostructures. Next, 600 sccm Ar was introduced at about 20 min. Then, the flow rate was reduced to 120 sccm and the furnace was heated to 1150 °C in 35 min. When the temperature reached to 1150 °C, the direction of Ar gas was changed and kept for 0–40 s. Then we used magnets and quartz hooks to pull the boat out quickly and turned the air flow back into the reverse direction. At last, the reactor was cooled to room temperature.

2.3. Synthesis of 2D/1D WS_2/MoS_2 heterostructures

Similarly, MoS_2 powders were placed in the center of the heat zone and the SiO_2/Si substrate with WS_2 nanosheets was placed at the downstream. Next, 600 sccm Ar was introduced. Then, the flow rate was reduced to 120 sccm and the furnace was heated to 1190 °C in 40 min. When the temperature reached to 1190 °C, the direction of Ar gas was changed and kept for 0.5–3 min. Then we used magnets and quartz hooks to pull the boat out quickly and turned the air flow back into the reverse direction. At last, the reactor was cooled to room temperature.

2.4. Material characterization

The Raman and PL spectra images were conducted via a laser micro-Raman spectrometer (Renishaw Invia). The width of the heterostructure was measured by AFM (Bruker model: Dimension ICON) and SEM (TESCAN MIRA3).

3. Result and discussion

As shown in Fig. 1, we modified a bidirectional flow CVD process to precisely control the growth process that has been reported[20]. In this system, reverse gas flow (green arrow) was introduced during the heating stage, which can clean the quartz tube and avoid unwished for source deposition. Compared with the forward flow, the reverse flow passes through the substrate at a lower temperature, which can avoid thermal etching in the heating process. The direction of air flow was transformed (red arrow) quickly when reaching the growth temperature. Moreover, when the growth process stops, the substrate was pulled out and the airflow reverses again. For 1D WSe_2 growth, when we pull the boat out and reverse the direction of the gas, the growth process can be terminated completely and immediately.

Because the heat resistance of WS_2 is better than that of WSe_2, we choose WS_2 as the growth substrate. As shown in Fig. 2(a), monolayer WS_2 that we synthesized in the first step is about 100 μm. The uniform surface and sharp edge are suitable for the epitaxy of the second step. Fig. 2(b) shows that PL peak of monolayer WS_2 locates at 640 nm, which is consistent with previous study[20, 21]. As shown in Fig. 2(c), there are two distinct peaks at 357 and 419 cm^{-1}, which can be assigned to the E' and A_1' modes, respectively[22]. The sharp edge and uniform surface of WS_2 facilitate epitaxial growth. The PL mapping images at 640 nm and Raman mapping images at 357 cm^{-1} are shown in Figs. 2(e) and 2(f). The uniform color represents the high quality and uniformity of monolayer WS_2, which laid a good foundation for the next step of growth.

As shown in Fig. 3, the width of WSe_2 of the WS_2/WSe_2 heterostructures can be sequentially tuned by controlling the air direction and growth time. When the growth time is controlled at 5 s, the WSe_2 nanoribbons can be grown at the edge of WS_2 with a width of 90 nm (Fig. 3(a)), which means that the 2D/1D WS_2/WSe_2 heterostructure is synthesized. With the prolongation of growth time, the width of WSe_2 is increased to a few hundred nanometers (Figs. 3(b)–3(d)). As shown in Figs. 3(e) and 3(f), the width of WSe_2 can be tuned larger than 1 μm when the growth time is 30 s. Moreover, it can be observed that the WS_2/WSe_2 heterostructures are clean and uniform, which are good for application.

In fact, there are some narrower nanoribbons at 0–3 s that are difficult to be characterized by AFM, so we conducted scanning electron microscopy (SEM) to characterize their widths. As shown in Fig. 4, the 11 nm wide WSe_2 can be grown at the edge of WS_2, which represents that an ultra-narrow nanowire was synthesized.

To prove the universality of this approach, 2D/1D WS_2/MoS_2 lateral heterostructures were also synthesized by using the same method. Fig. 5(a) shows that the width of MoS_2 is about 4 μm when the growth time is 3 min. When the growth time is reduced to 1 min, the width of MoS_2 is reduced to 300 nm (Fig. 5(b)). As shown in Fig. 5(c), the width of MoS_2 is reduced to 200 nm with the growth time reduced to 30 s. These results show that our method can control the width of a 2D/1D heterostructure simply and effectively.

The Raman and PL analyses were conducted to further study the spectroscopy and photoluminescence performance of the as-grown lateral heterostructure. Fig. 6(a) shows the Raman spectra at three different locations of the WS_2, WS_2/MoS_2 interface and MoS_2. Two distinct peaks at 357 and 419 cm^{-1} in the Raman spectrum of WS_2 (blue line) are consistent with those mentioned above. The Raman spectrum from the peripheral region display two peaks at 384 and 405 cm^{-1} (red line in Fig. 6(a)), in agreement with the E' and A_1' resonance modes of MoS_2[23], respectively. As expected, four peaks appear in the corresponding Raman spectrum of the WS_2/MoS_2 interface, indicating mixed Raman signals of both WS_2 and MoS_2. The PL spectra (Fig. 6(b)) acquired from the monolayer WS_2 (blue line) and MoS_2 (red line) show strong peaks at wavelengths of 633 and 670 nm, respectively, corresponding to the direct excitonic transition energy in monolayer WS_2 and MoS_2. The mixed peaks at 634 and 668 nm of the interface (black line) can be attributed to WS_2 and MoS_2, respectively. In the same way, the Raman and PL spectra of the

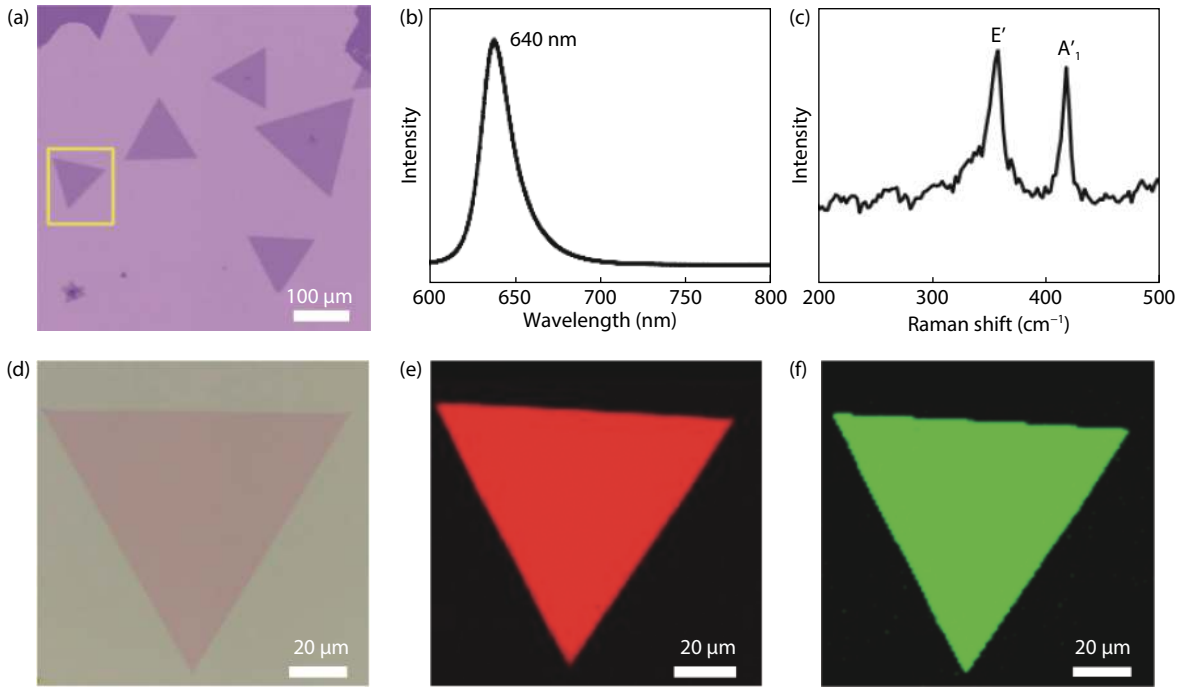

Fig. 2. (Color online) (a) Optical image of monolayer WS_2. (b) PL spectrum of WS_2. (c) Raman spectrum of WS_2. (d) Optical image of WS_2 in the yellow rectangle of (a). (e) PL mapping image of monolayer WS_2. (f) Raman mapping image of monolayer WS_2.

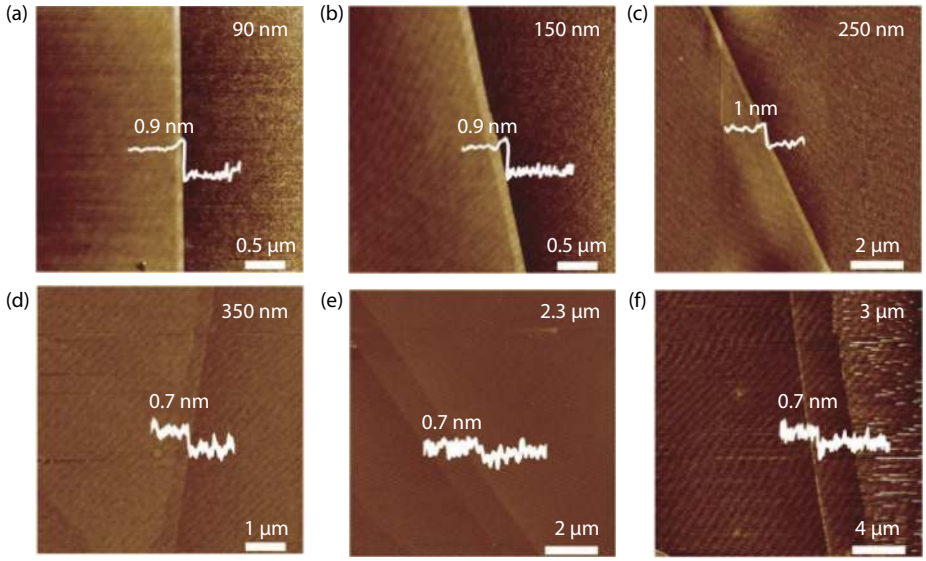

Fig. 3. (Color online) AFM images of WS_2/WSe_2 lateral heterostructure when the growth time are (a) 5 s, (b) 7 s, (c) 9 s, (d) 11 s, (e) 30 s and (f) 40 s.

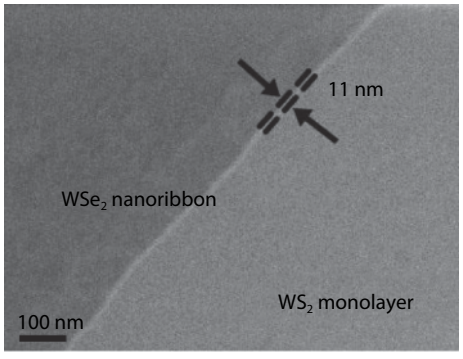

Fig. 4. SEM image of the 2D/1D WS_2/WSe_2 lateral heterostructure.

WS_2/WSe_2 heterostructure are shown in Figs. 6(c) and 6(d). The Raman spectrum of WS_2/WSe_2 shows three distinct peaks at 257, 356, 413 cm^{-1}, which are consistent with the Raman spectrum of monolayer WSe_2 and WS_2. The mixed PL signals (Fig. 6(d)) also can be observed at the interface of WS_2/WSe_2.

4. Conclusion

In summary, we successfully synthesized 2D/1D WS_2/WSe_2 (WS_2/MoS_2) lateral heterostructures by a bidirectional flow CVD reactor. WSe_2 and MoS_2 with different widths can be epitaxially grown on the edge of WS_2. The width of the WSe_2 can be tuned from 11 nm to 4 μm by precisely con-

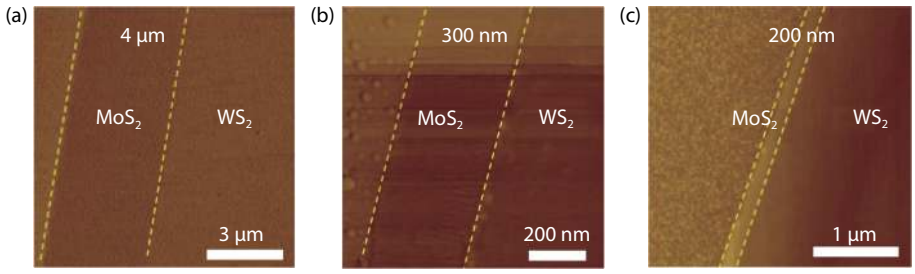

Fig. 5. (Color online) AFM phase image of WS_2/MoS_2 lateral heterostructure when the growth time are (a) 3 min, (b) 1 min, and (c) 30 s.

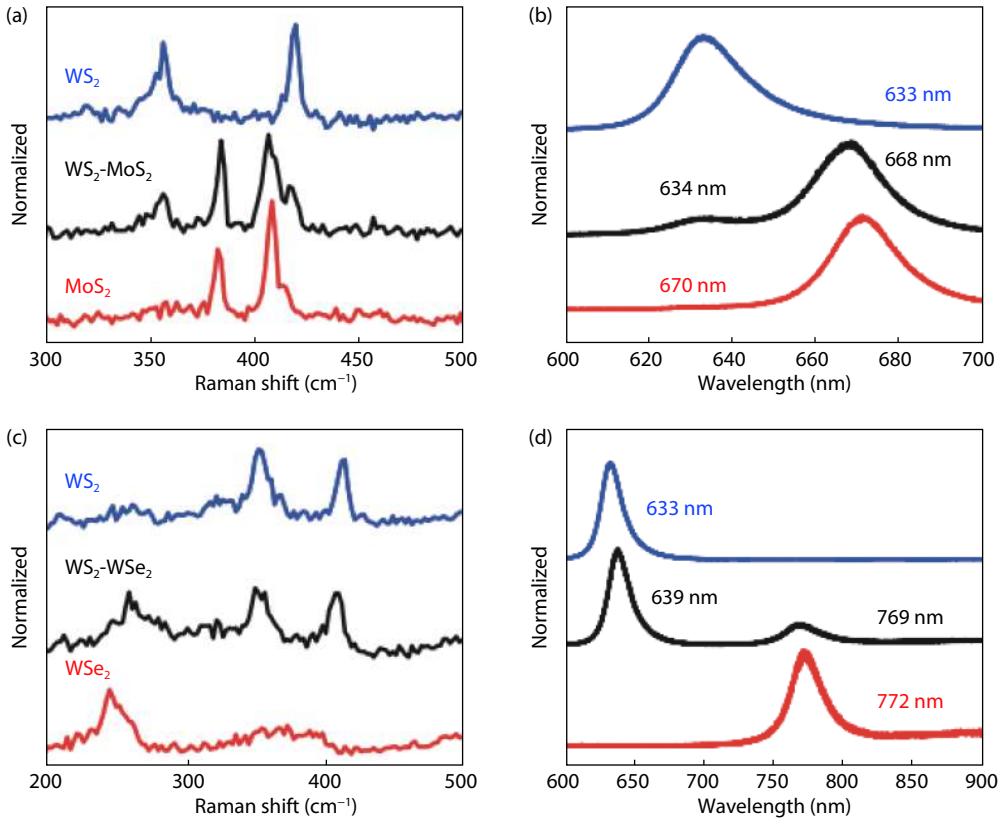

Fig. 6. (Color online) Raman and PL spectrum of WS_2/MoS_2 and WS_2/WSe_2 heterostructures. (a) Raman spectrum of the WS_2/MoS_2 heterostructure. (b) PL spectrum of the WS_2/MoS_2 heterostructure. (c) Raman spectrum of the WS_2/WSe_2 heterostructure. (d) PL spectrum of the WS_2/WSe_2 heterostructure.

trolling the growth time. AFM and SEM images show that the interface of the 2D/1D heterostructures is clear and smooth. Our investigation provides a new method for the preparation of ultranarrow 1D nanoribbons and breaks new ground in the future study of the 2D/1D lateral heterostructures.

Acknowledgements

The authors at Hunan University acknowledge the support from National Natural Science Foundation of China (No. 51872086), the Hunan Key Laboratory of Two-Dimensional Materials (Grant No. 2018TP1010) and the Innovative Research Groups of Hunan Province (Grant No. 2020JJ1001) for the work conducted at Hunan University.

References

[1] Trentler T J, Hickman K M, Goel S C, et al. Solution-liquid-solid growth of crystalline III-V semiconductors: an analogy to vapor-liquid-solid growth. Science, 1995, 270(5243), 1791

[2] Yan R, Gargas D, Yang P. Nanowire photonics. Nat Photon, 2009, 3(10), 569

[3] Zheng L X, O'Connell M J, Doorn S K, et al. Ultralong single-wall carbon nanotubes. Nat Mater, 2004, 3(10), 673

[4] Lei S, Ge L, Najmaei S, et al. Evolution of the electronic band structure and efficient photo-detection in atomic layers of InSe. Acs Nano, 2014, 8(2), 1263

[5] Poh S M, Tan S J R, Zhao X, et al. Large area synthesis of 1D-$MoSe_2$ using molecular beam epitaxy. Adv Mater, 2017, 29(12), 1605641

[6] Qi R, Wang S, Wang M, et al. Towards well-defined MoS_2 nanoribbons on a large scale. Chem Commun, 2017, 53(70), 9757

[7] Li S, Lin Y C, Zhao W, et al. Vapour-liquid-solid growth of monolayer MoS_2 nanoribbons. Nat Mater, 2018, 17(6), 535

[8] Huang W, Wang X, Ji X, et al. In-situ fabrication of Mo_6S_6-nanowire-terminated edges in monolayer molybdenum disulfide. Nano Res, 2018, 11(11), 5849

[9] Zhou Y, Dong J, Li H, et al. Electronic transport properties of in-plane heterostructures constructed by MoS_2 and WS_2 nanoribbons. RSC Adv, 2015, 5(82), 66852

[10] Zhou W, Yu G, Rudenko A N, et al. Tunable half-metallicity and

edge magnetism of H-saturated InSe nanoribbons. Phys Rev Mater, 2018, 2(11), 114001
[11] Chen K X, Luo Z Y, Mo D C, et al. WSe_2 nanoribbons: new high-performance thermoelectric materials. Phys Chem Chem Phys, 2016, 18(24), 16337
[12] Wu M, Shi J J, Zhang M, et al. Modulation of electronic and magnetic properties in InSe nanoribbons: edge effect. Nanotechnology, 2018, 29(20), 205708
[13] Magda G Z, Jin X, Hagymasi I, et al. Room-temperature magnetic order on zigzag edges of narrow graphene nanoribbons. Nature, 2014, 514(7524), 608
[14] Wang J J, Cao F F, Jiang L, et al. High performance photodetectors of individual InSe single crystalline nanowire. J Am Chem Soc, 2009, 131(43), 15602
[15] Yu Y, Wang G, Tan Y, et al. Phase-controlled growth of one-dimensional Mo_6Te_6 nanowires and two-dimensional $MoTe_2$ ultrathin films heterostructures. Nano Lett, 2018, 18(2), 675
[16] Zhang J, Wei Y, Yao F, et al. SWCNT-MoS_2-SWCNT vertical point heterostructures. Adv Mater, 2017, 29(7), 1604469
[17] Jariwala D, Sangwan V K, Wu C C, et al. Gate-tunable carbon nanotube-MoS_2 heterojunction p-n diode. Proc Natl Acad Sci USA, 2013, 110(45), 18076
[18] Liu Y, He X, Hanlon D, et al. Liquid phase exfoliated MoS_2 nanosheets percolated with carbon nanotubes for high volumetric/areal capacity sodium-ion batteries. Acs Nano, 2016, 10(9), 8821
[19] Huang H, Huang W, Yang Z, et al. Strongly coupled MoS_2 nanoflake-carbon nanotube nanocomposite as an excellent electrocatalyst for hydrogen evolution reaction. J Mater Chem A, 2017, 5(4), 1558
[20] Zhang Z, Chen P, Duan X, et al. Robust epitaxial growth of two-dimensional heterostructures, multiheterostructures, and superlattices. Science, 2017, 357(6353), 788
[21] Duan X, Wang C, Shaw J C, et al. Lateral epitaxial growth of two-dimensional layered semiconductor heterojunctions. Nat Nanotechnol, 2014, 9(12), 1024
[22] Berkdemir A, Gutierrez H R, Botello-Mendez A R, et al. Identification of individual and few layers of WS_2 using Raman Spectroscopy. Sci Rep, 2013, 3, 1755
[23] van der Zande A M, Huang P Y, Chenet D A, et al. Grains and grain boundaries in highly crystalline monolayer molybdenum disulphide. Nat Mater, 2013, 12, 554

Di Wang received her bachelor's degree from Qufu Normal University in 2018. She continued her master studies at Hunan University under the guidance of Prof. Xidong Duan. Her research interests are in the field of two-dimensional (2D) materials and their electrochemistry.

Xidong Duan is a research scientist at the College of Chemistry and Chemical Engineering, Hunan University, China. His current research interests include two-dimensional materials, heterostructures, superlattices and their applications. He received his BS, MA and PhD degrees from Hunan University. He is the Yangtze River scholar professor and published more than 40 papers including *Nature* and *Science* as the first or corresponding author.